

The Invariant Twist of Magnetic Fields in the Relativistic Jets of Active Galactic Nuclei

Ioannis Contopoulos,¹ Dimitris M. Christodoulou,²
Demosthenes Kazanas,³ and Denise C. Gabuzda⁴

ABSTRACT

The origin of cosmic magnetic (\mathbf{B}) fields remains an open question. It is generally believed that very weak primordial \mathbf{B} fields are amplified by dynamo processes, but it appears unlikely that the amplification proceeds fast enough to account for the fields presently observed in galaxies and galaxy clusters. In an alternative scenario, cosmic \mathbf{B} fields are generated near the inner edges of accretion disks in Active Galactic Nuclei (AGNs) by azimuthal electric currents due to the difference between the plasma electron and ion velocities that arises when the electrons are retarded by interactions with photons. While dynamo processes show no preference for the polarity of the (presumably random) seed field that they amplify, this alternative mechanism uniquely relates the polarity of the poloidal \mathbf{B} field to the angular velocity of the accretion disk, resulting in a unique direction for the toroidal \mathbf{B} field induced by disk rotation. Observations of the toroidal fields of 29 AGN jets revealed by parsec-scale Faraday rotation measurements show a clear asymmetry that is consistent with this model, with the probability that this asymmetry came about by chance being less than 1%. This lends support to the hypothesis that the Universe is seeded by \mathbf{B} fields that are generated in AGN via this mechanism and subsequently injected into intergalactic space by the jet outflows.

¹Research Center for Astronomy, Academy of Athens, Athens 11527, Greece.

Email: icontop@academyofathens.gr

²Dept. of Mathematical Sciences, University of Massachusetts Lowell, Lowell 01854.

E-mail: dimitris_christodoulou@uml.edu

³NASA/GSFC, Code 663, Greenbelt, MD 20771.

E-mail: demos.kazanas@nasa.gov

⁴Dept. of Physics, University College Cork, Cork, Ireland.

Email: gabuzda@physics.ucc.ie

1. Introduction

Despite progress, the origin of cosmic magnetic (\mathbf{B}) fields remains an open question (Carilli & Taylor 2002; Widrow 2002; Kronberg 2005; Kulsrud & Zweibel 2008; Bernet et al. 2008). The general view is that initially weak ($\sim 10^{-20}$ G) \mathbf{B} fields generated by the “Biermann battery” (Biermann 1950) are amplified to the observed mean galactic values ($\sim 10^{-6}$ G) by dynamo processes. However, it is not clear how the dynamo mechanism can achieve the observed large-scale separation of the opposing field polarities, especially in view of flux-freezing, which hinders field diffusion (Kulsrud & Zweibel 2008). This problem is particularly acute for galaxies and galaxy clusters, which already have well-developed, ordered \mathbf{B} fields at redshifts of $z \simeq 2 - 3$.

An alternative mechanism for the generation and amplification of \mathbf{B} fields is the “Poynting–Robertson (PR) cosmic battery,” which has been proposed to operate in AGNs (Contopoulos & Kazanas 1998; Contopoulos, Kazanas & Christodoulou 2006; Christodoulou, Contopoulos & Kazanas 2008). In this model, radiation from the active nucleus appears slightly anisotropic in the rest frame of the accretion disk rotating about the central supermassive black hole (BH) due to aberration. This gives rise to a PR drag force that is inversely proportional to the square of the particle mass, and so acts predominantly on the disk electrons, decreasing their velocities relative to those of the disk protons.¹ This generates azimuthal electric currents in the direction of disk rotation, which, in turn, give rise to a poloidal field B_P whose direction is directly related to the direction of the disk rotation. The PR current source is much stronger than that of the Biermann battery, and furthermore implies a direct coupling between accretion-flow vorticity, disk-plasma diffusivity, and the generated large-scale, ordered \mathbf{B} field (Contopoulos & Kazanas 1998; Contopoulos et al. 2006; Christodoulou et al. 2008; see also Kulsrud et al. 1997 for the role of fluid vorticity).

All that is required for this mechanism to operate is the presence of (i) radiation from the central AGN and (ii) a surrounding rotating accretion disk. Although Contopoulos & Kazanas (1998) assumed a central isotropic radiation field and an advection-dominated accretion flow, the action of the PR battery does not depend on the particular geometry or properties of the AGN or accretion disk. Note also that the PR battery is a large-scale, secular effect that is independent of (and certainly does not preclude) the presence of small-scale \mathbf{B} fields and magneto-rotational instability in the accretion disk.

In our scenario, \mathbf{B} -field loops generated by the PR battery and anchored in the inner and

¹From the observer’s viewpoint, this force appears when the nuclear radiation, which is re-radiated isotropically in the rest frame of the electrons, is beamed in the direction of motion, i.e., in the direction of the disk rotation.

outer accretion disk become twisted in the azimuthal direction by the differential rotation of the disk. As their twisting relaxes in the vertical direction, the loops open up and separate into an “inner” component near the disk symmetry axis and an “outer” component (the “return field”) threading the disk farther from the axis. The poloidal fields B_P of the two components are in opposite directions, one parallel and the other antiparallel to the angular velocity vector ω .

In a general MHD picture, the direction of disk rotation and the polarity of the “wound-up” \mathbf{B} fields are unrelated. However, in the PR battery, the direction of B_P is uniquely determined by the direction of the disk rotation; thus, *the associated jets should have a near-axis B_P that is parallel to ω and an extended B_P with the opposite polarity in the surrounding accretion disk, with each component carrying the same magnetic flux.* As we will now see, this coupling of the polarity of B_P and disk rotation results in invariant directions for the toroidal components of the inner (near-axis) and outer (return fields), both of which are wound up by the disk rotation.

2. The PR Cosmic Battery and Faraday Rotation

In the PR battery, an overall helical \mathbf{B} field is produced when the bases of initially poloidal field lines are dragged by the rotating disk plasma, with the inner B_T pointing opposite to the direction of disk rotation in the northern (N) hemisphere of the disk and in the direction of disk rotation in the southern (S) hemisphere (Fig. 1a); the opposite is true for the return field farther out in the accretion disk (Fig. 1b). Fig. 1 illustrates a unique feature of the PR battery: *reversing the observer’s hemisphere, or equivalently, the direction of disk rotation, reverses B_P , but leaves the direction of B_T unchanged in the observer’s sky* (red \mathbf{B} -field arrows in Fig. 1).

This can be tested for AGN jets, where the direction of B_T can be directly inferred from the direction of FR gradients transverse to the jet axis (Blandford 1993). FR is a rotation of the plane of linear polarization that occurs when the polarized radiation passes through a magnetized plasma. The rotation of the polarization angle χ is determined by the observing wavelength λ , the density of free electrons n_e , and the line-of-sight component of the \mathbf{B} field in the plasma, B_{LOS} :

$$\chi = \chi_0 + \frac{e^3 \lambda^2}{8\pi \epsilon_0 m_e^2 c} \int n_e(s) \vec{B}(s) \cdot d\vec{s} \equiv \chi_0 + (\text{RM}) \lambda^2, \quad (1)$$

where χ_0 is the intrinsic polarization angle, e the electron charge, m_e the electron mass, ϵ_0 the dielectric constant, c the speed of light, and RM the rotation measure. The integral is

taken over the line of sight from the source to the observer. Upper limits to n_e of a few times 10^4 cm^{-3} are set by the requirement that the optical depth for free-free absorption be less than unity (assuming a Faraday screen depth of one parsec -the same as that seen on the plane of the sky, and a temperature of 10^4 K). RMs of 1000 rad m^{-2} in quasar cores to a few hundred rad m^{-2} for quasar jets imply fields of 3 to $0.3 \mu\text{G}$ (Zavala & Taylor 2003). The sign of the RM is determined by the direction of B_{LOS} , with B_{LOS} directed toward the observer being positive. The presence of a helical jet \mathbf{B} field gives rise to a transverse FR gradient, due to the systematic change in B_{LOS} across the jet. The PR battery predicts that *the FR due to the inner region of helical \mathbf{B} field should always increase in the CW direction on the sky, and the FR due to the outer, return field in the CCW direction, relative to the jet origin*. This arises due to the unique twisting of the inner and outer helical fields generated by the PR battery (Fig. 1).

The direction of the net observed transverse FR gradient will be determined by which region of helical field dominates the FR integral. This will be determined by factors such as the fall-off of the electron density and \mathbf{B} field with distance from the jet axis and the AGN center and the opening angle and viewing angle of the jet. If the inner (outer) helical field tends to dominate the observed FR, this should lead to an excess of CW (CCW) transverse FR gradients relative to the jet origins on the corresponding scales. In contrast, if the initial poloidal field is random, there should be equal numbers of CW and CCW gradients within the statistical errors. Note that the FR associated with the inner region of helical field need not be internal FR, since it may occur predominantly in a sheath layer surrounding this region.

3. Faraday Rotation Data

We searched the literature for reliable transverse FR gradients detected across AGN jets on pc scales derived from multi-wavelength Very Long Baseline Interferometry (VLBI) polarimetry. We included only transverse FR gradients that are close to orthogonal to the local jet direction, monotonic across the jet, and extend across all or nearly all of the jet (this excludes cases where there is an enhancement or reduction in the local FR at one edge of the jet). This yielded the list of 29 AGN in Table 1, which indicates the AGN, its redshift, the rough distance from the VLBI core where the FR gradient is observed in milliarcseconds (mas) and in pc, whether the FR gradient is CW or CCW with respect to the jet origin, and references. FR-gradient distances given as zero are observed across the VLBI core region (the “core” corresponds to the optically thick base of the jet, and the jet origin is further “upstream” from the core; Blandford & Königl 1979). Most of these images were obtained

from 2–4 cm or 2–6 cm observations with the Very Large Baseline Array (VLBA), and so have comparable resolutions. The only exceptions are the 7 mm–2 cm image of 3C 120 of Gomez et al. (2008), 3.6–18 cm image of 1652+398 of Gabuzda (2006), and 18–22 cm image of 1749+701 of Hallahan & Gabuzda (2009). The case of 1803+784 is unique: while transverse FR gradients are present in both the core region and jet, the direction of the core gradient is constant, while the direction of the jet gradient changes with time (Mahmud, Gabuzda & Bezrukovs 2009). Therefore, we have included an entry for this object only for the core-region transverse FR gradient.

4. Results

Fig. 2 plots the distances from the VLBI core in pc for the transverse FR gradients listed in Table 1, with the results stacked vertically in order of right ascension. CW gradients are shown as circles, and CCW gradients as triangles. For 7 AGN for which transverse FR gradients are detected on two appreciably different scales, the larger-scale gradients are shown by hollow symbols.

Of the 36 total transverse FR gradients observed in these 29 AGN, 22 are CW and 14 CCW. A simple analysis using the binomial probability distribution

$$P = \sum_{N_{CW}}^N \frac{1}{2^N} \frac{N!}{N_{CW}!N_{CCW}!}, \quad (2)$$

(N_{CW} , N_{CCW} are the numbers of CW, CCW FR gradient measurements and $N = N_{CW} + N_{CCW}$) indicates that 22 or more CW gradients would come about by chance with a probability of about 12% ($N_{CW} = 22$, $N_{CCW} = 14$, $N = 36$). However, if we consider only the FR gradients detected closest to the VLBI core (i.e., those depicted using filled symbols in Fig. 2), we find 22 CW gradients and only 7 CCW gradients, with the probability of 22 or more CW gradients coming about by chance being only 0.4% ($N_{CW} = 22$, $N_{CCW} = 7$, $N = 29$)! In contrast, all 7 of the larger-scale FR gradients (depicted by the hollow symbols in Fig. 2) are CCW. The probability that all 7 of these 7 gradients are CCW by chance is also low, about 0.8% ($N_{CW} = 0$, $N_{CCW} = 7$, $N = 7$).

These results are consistent with the expectations of the PR battery model if the inner region of helical field dominates relatively close to the jet origin.

5. Discussion

5.1. Freedom from Observational Selection Effects

It is important to ensure that the observed asymmetry between the numbers of CW and CCW transverse FR gradients could not be an observational selection effect. Our key criterion for selecting the 29 AGN considered here is that their jets display monotonic FR gradients that are close to orthogonal to the local jet direction. We included all such cases, without regard to the direction of the observed FR gradients, other than the requirement that they be close to orthogonal to the jet. Thus, it would be essentially impossible to inadvertently introduce a bias between the numbers of CW and CCW gradients during our selection of the AGN for this study.

5.2. Potential for Deducing the Direction of Disk Rotation

The sign of the FR observed along the central “spine” of the jet is determined by the direction of the dominant poloidal field B_P and the viewing angle θ . Let us suppose that B_P is generated by the PR battery and that the inner region of helical field is usually dominant. When viewed from the N hemisphere of the accretion disk, B_P will be directed toward the observer if θ is less than $1/\gamma$, where γ is the Lorentz factor of the jet (i.e., the viewing angle is less than 90° in the rest frame of the jet), and away from the observer if θ is greater than $1/\gamma$. Since the PR battery requires that B_P is parallel to ω in the inner region of the accretion disk, the direction of B_P corresponds directly to the direction of rotation of the disk. If θ is less than $1/\gamma$, positive, on average, FR values along the jet “spine” indicate that the inner B_P points toward the observer, who then must be located in the N hemisphere of the disk (as in Fig. 1a), which accordingly rotates CCW on the sky. Similarly, if θ is less than $1/\gamma$, negative, on average, FR values indicate that the observer is located in the S hemisphere of the disk (as in Fig. 1b), which rotates CW on the sky.

Unfortunately, it is not possible to be certain whether a jet’s viewing angle is less than or greater than $1/\gamma$, although the most likely viewing angle is $\simeq 0.6\gamma$ (Kellermann et al. 2004). For two objects in which the sense of rotation of the underlying accretion disk is known, our model is in agreement with the observed Faraday-rotation signs if these jets are viewed at angles of less than $1/\gamma$. HST direct imaging of the M87 nucleus (Tsvetanov et al. 1999) and maser emission in the inner disk of NGC 4258 (Hernstein et al. 2007) reveal that the accretion disks in these systems rotate CW on the sky. FR measurements along the jet spine in M87 (Zavala & Taylor 2002) and in NGC 4258 (Krause & Lohr 2004) yield large negative FR values (B_{LOS} directed away from the observer). Thus, in the PR battery

model, an observer viewing the jet at an angle of less than $1/\gamma$ would be located in the S hemisphere (Fig. 1b), and these two accretion disks should indeed be rotating CW on the sky. Naturally, more such cases must be tested before it will be possible to determine if this agreement provides further evidence for the action of the PR battery in AGN.

5.3. Energy Budgets of AGN

The total magnetic energy content of the kpc-scale lobes of extragalactic radio sources can reach $\sim 10^{60} - 10^{61}$ erg (Kronberg et al. 2001; Carilli & Taylor 2002; Widrow 2002; Kronberg 2005; Kulsrud & Zweibel 2008). If the PR-battery-generated \mathbf{B} fields remain near equipartition at distances R of the order of the BH event horizon, this energy is comparable to the Poynting flux produced by the twisting of this \mathbf{B} field ($\sim B^2 R^2 c$) over the AGN lifetime ($10^8 - 10^9$ yrs). This is also of the same order as the energy released by the gravitational infall of matter onto the BH, implying that AGN convert a significant fraction of their accretion luminosity into Poynting flux, which, in turn, feeds their radio lobes with magnetic energy.

6. Conclusions

We have found an asymmetry in the directions of FR gradients observed across AGN jets that is difficult to explain using standard models for AGN jet \mathbf{B} fields, in which a toroidal field is generated when an initially random poloidal field anchored in the accretion disk is wound up by the differential rotation of the disk. The reason for this is simple: there should be no preference for either the direction of the disk rotation or the direction of the initial (“seed”) poloidal field. This means that, although the toroidal field that is generated in a particular AGN jet will have a particular direction, there should be no preferred direction for AGN jets as a whole.

The CW/CCW Faraday-rotation gradient asymmetry we have discovered requires some mechanism that couples the sense of rotation of the accretion disk to the direction of the poloidal field, and the PR cosmic battery provides precisely such a mechanism. The observed preference for CW FR gradients finds a natural explanation if the poloidal fields are generated by the PR battery, and the inner, near-axis helical \mathbf{B} field dominates the FR integrals in most observed AGN jets on pc scales, with the outer field being on occasion dominant farther from the jet origin. The relatively few jets that exhibit only CCW transverse FR gradients can be understood as corresponding to the outer region of the helical \mathbf{B} field, with the region of inner helical B field dominance being on scales smaller than the resolution of the VLBI

observations. Our main conclusions can be summarized as follows:

1. In the PR battery model, the direction of B_P threading the inner part of the accretion disk in AGN is parallel to ω . The resulting FR (B_T) gradient near the jet base has a unique direction projected onto the sky, increasing in the CW direction relative to the origin of the jet, independent of the direction of disk rotation. We find remarkable support for this picture: 22 of 29 transverse pc-scale FR gradients observed closest to the VLBI cores are CW, while only 7 are CCW, with the probability of this occurring by chance being only 0.4%.
2. In all 7 AGN in which transverse FR gradients were observed at two different distances from the VLBI core, the FR gradients farther from the core are CCW, suggesting that these are regions where the outer helical \mathbf{B} field dominates the total observed FR. This also suggests the existence of a transition distance, within which the inner region and beyond which the outer region of helical fields tend to dominate.
3. The collected pc-scale FR observations strengthen the view that AGN jets have helical \mathbf{B} fields and are primarily magnetically driven.
4. Since the total polarization rotations due to the observed FR exceed $\simeq 45^\circ$ ($\simeq 1$ rad) in some cases (e.g. 3C371: Gabuzda et al. 2004; 3C78: Kharb et al. 2009), the FR in these sources must be external (Burn 1966). This suggests that the FR due to the inner region of helical field arises in a sheath surrounding that region, as was also proposed by Kharb et al. (2009). FR associated with the outer region of helical field is, of course, external.
5. If \mathbf{B} fields are indeed produced by the PR battery in AGN jet–disk systems and are then carried outward along jet outflows and ultimately expelled into intergalactic space, these fields should make a substantial contribution to the intergalactic \mathbf{B} fields.

It may be premature to state that the predominance of CW transverse FR gradients we have found conclusively demonstrates that the PR battery mechanism operates in the accretion disk–jet systems of AGN. At the same time, these surprising results are difficult to explain using any standard MHD model in the literature, and seem to require a physical mechanism that couples the directions of the disk rotation and the poloidal \mathbf{B} field, as is the case for the PR cosmic battery.

We are currently undertaking numerical studies to investigate the conditions required for the inner region of helical \mathbf{B} field to dominate on relatively small scales, with a transition to dominance of the outer region of helical field at some distance along the jet. We hope

that comparison of these numerical results with observations will provide fundamentally new insight into the inherent structures of AGN jets.

We acknowledge useful discussions with Russell Kulsrud, Ramesh Narayan, and Iossif Papadakis, and useful feedback from an anonymous referee.

REFERENCES

- Asada K., Inoue M., Uchida Y., Kamenno S., Fujisawa K., Iguchi S., Mutoh M. 2002, PASJ, 54, L39
- Asada K., Inoue M., Nakamura M., Kamenno S., Nagai H. 2008, ApJ, 682, 798
- Bernet M. L., Miniati F., Lilly S. J., Kronberg P. P., Dassauges–Zavadsky M., Nature, 454, 302
- Biermann L. 1950, Naturforsch., 5a, 65
- Blandford R.D. 1993, in *Astrophysical Jets* (Cambridge: Cambridge Univ. Press), p. 26
- Blandford R.D. & Königl A. 1979, ApJ, 232, 34
- Burn B.J. 1966, MNRAS, 133, 67
- Christodoulou D. M., Contopoulos I., Kazanas D. 2008, ApJ, 674, 388
- Contopoulos I. & Kazanas D. 1998, ApJ, 508, 859
- Contopoulos I., Kazanas D., Christodoulou D. M. 2006, ApJ, 652, 1451
- Carilli C. L. & Taylor G. B. 2002, Ann. Rev. Astron. Astrophys., 40, 319
- Gabuzda D. 2006, in *Proceedings of the 8th European VLBI Network Symposium*, http://pos.sissa.it//archive/conferences/036/011/8thEVN_011.pdf
- Gabuzda D. C., Murray É., Cronin P. 2004, MNRAS, 351, L89
- Gabuzda D. C., Vitrichchak V. M., Mahmud M., O’Sullivan S. P. 2008, MNRAS, 384, 1003
- Gómez J. L., Marscher A. P., Jorstad S. G., Agudo I., Roca–Sogorb M. 2008, ApJ, 681, L69
- Hallahan R. & Gabuzda D. C. 2009, in *Proceedings of the 9th EVN Symposium*, in press (Proceedings of Science, 2009)

- Hernstein, J. R., Moran, J. M., Greenhill, L. J. & Trotter, A. S. 2007, *ApJ*, 629, 719
- Kellermann K.I., Lister M.L., Homan D.C., Vermeulen R.C., Cohen M.H., Ros E., Kadler M, Zensus J.A. & Kovalev Y.Y. 2004, *ApJ*, 609, 539
- Kharb P., Gabuzda D.C., O’Dea C.P., Shastri P. & Baum S.A. 2009, *ApJ*, 694, 1485
- Krause, M. & Lohr, A. 2004, *A& A*, 420, 115
- Kronberg P. P. 2005, in *Cosmic Magnetic Fields, Lecture notes in Physics*, R. Wielebinski and R. Beck (Eds.), 664, 9 (Springer: Berlin 2005)
- Kronberg P. P., Dufton Q. W., Li H., Colgate S. A. 2001, *ApJ*, 560, 178
- Kulsrud R. M., Cen R., Ostriker J. P., Ryu D. 1997, *ApJ*, 480, 481
- Kulsrud R. M & Zweibel E. G. 2008, *Rep. Prog. Phys.*, 71, 046901, doi:10.1088/0034-4885/71/4/046901
- Mahmud M. & Gabuzda D. 2008, in *Extragalactic Jets: Theory and Observations from Radio to Gamma Ray*, ASP Conf. Ser., 386, 494
- Mahmud M. & Gabuzda D. C. 2009, in *Proceedings of the 9th EVN Symposium (Proceedings of Science, 2009)*; http://pos.sissa.it/archive/conferences/072/011/IX%20EVN%20Symposium_011.pdf
- Mahmud M., Gabuzda D. C. & Bezrukovs V. 2009, *MNRAS*, in press; arXiv:astro-ph/0905.2368
- O’Sullivan S.P. & Gabuzda D. C. 2009, *MNRAS*, 393, 429
- Taylor G. B. 1998, *ApJ*, 506, 637
- Taylor G. B. 2000, *ApJ*, 533, 95
- Tsvetanov, Z. I., Allen, M. G., Ford, H. C. & Harms, R. J., in *The Radio Galaxy Messier 87*, H.-J. Röser & K. Meisenheimer (eds.), 301 (Berlin: Springer 1999)
- Widrow L. M., *Rev. Mod. Phys.*, 74, 775
- Zavala R. T. & Taylor G. B. 2002, *ApJ*, 566, L9
- Zavala R. T. & Taylor G. B. 2003, *ApJ*, 589, 126
- Zavala R. T. & Taylor G. B. 2004, *ApJ*, 612, 749

Zavala R. T. & Taylor G. B. 2005, ApJ, 625, L73

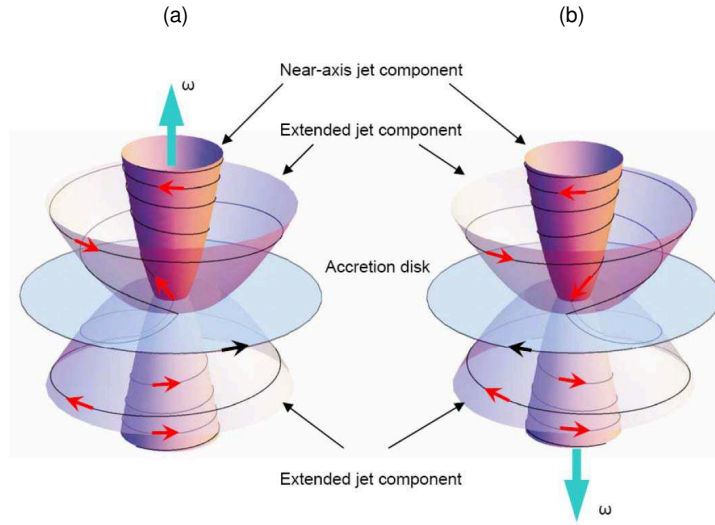


Fig. 1.— Sketch of an AGN jet \mathbf{B} field generated by the PR battery (black lines with red arrows) near the axis and periphery of the jet. The direction of disk rotation is shown by the black arrows in the disk and the corresponding angular velocity vector by the cyan arrows. The observer is located in the (a) northern and (b) southern hemisphere of the disk.

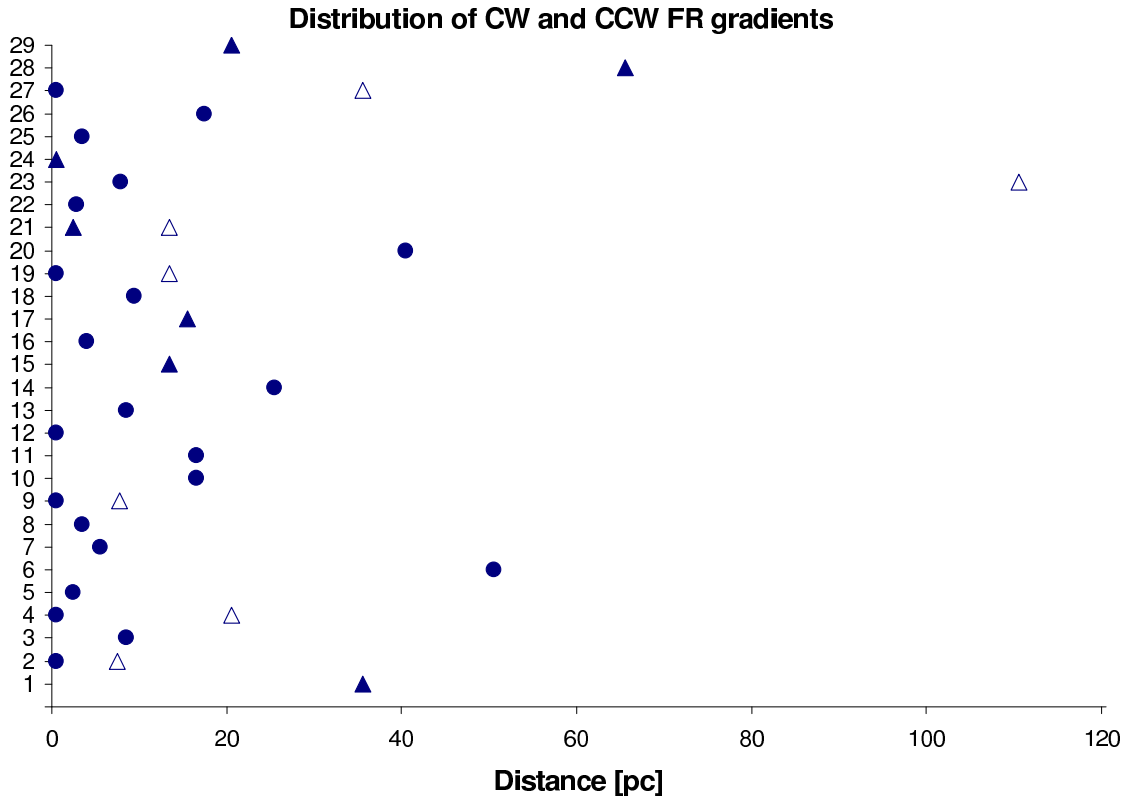


Fig. 2.— Distribution of transverse FR gradient directions relative to the jet origin in the plane of the sky; the numbers correspond to those in Table 1. CW/CCW gradients are denoted with circles/triangles, respectively. Open symbols are used for the farther gradient in objects where FR gradients are detected on two different scales.

Table 1. AGN Jets with Transverse FR Gradient Measurements

Source Number	Object	Alt. Name	z	pc/mas	Distance (mas)	Distance (pc)	Direction of FR Gradient	Refs.
1	0003-066		0.35	4.91	7	35	CCW	9
2	0138-097		0.733	7.26	0	0	CW	10
					1	7	CCW	
3	0212+735		2.37	8.16	1	8	CW	15
4	0256+075		0.90	7.79	0	0	CW	10
					2.5	20	CCW	
5	0305+039	3C78	0.029	0.57	4	2	CW	19
6	0333+321	NRAO140	1.259	8.35	6	50	CW	2
7	0415+379	3C111	0.05	0.96	5	5	CW	14
8	0430+052	3C120	0.03	0.66	4	3	CW	7
9	0716+714		0.31	4.56	0	0	CW	10
					1.5	7	CCW	
10	0735+178	DA237	> 0.42	> 5.4	3	> 16	CW	6
11	0745+241		0.41	5.45	3	16	CW	4
12	0748+126		0.889	7.76	0	0	CW	16
13	0820+225		0.95	7.9	10	8	CW	4
14	0836+710	4C71.07	2.218	8.25	3	25	CW	3
15	0954+658		0.37	5.09	2.5	13	CCW	9,11
16	1156+295	4C29.45	0.73	7.26	0.5	3.5	CW	6
17	1226+023	3C273	0.16	2.73	5	15	CCW	1,17
18	1253-055	3C279	0.54	6.33	1.5	9	CW	16
19	1334-127	OP158.3	0.54	6.35	0	0	CW	10
					2	13	CCW	
20	1641+399	3C345	0.59	6.65	6	40	CW	12
21	1652+398	Mrk501	0.03	0.66	3	2	CCW	4
					20	13	CCW	5
22	1749+096	4C09.57	0.32	4.67	0.5	2.3	CW	6
23	1749+701		0.77	7.41	1	7.4	CW	8,10
					15	110	CCW	
24	1803+784		0.68	7.06	0	0	CCW	15, 18

Table 1—Continued

Source Number	Object	Alt. Name	z	pc/mas	Distance (mas)	Distance (pc)	Direction of FR Gradient	Refs.
25	1807+398	3C371	0.05	0.97	3	3	CW	4
26	2005+403		1.74	8.46	2	17	CW	15
27	2155-152		0.67	7.03	0	0	CW	10
					5	35	CCW	
28	2230+114	CTA102	1.04	8.08	8	65	CCW	13
29	2251+158	3C454.3	0.86	7.68	2.5	20	CCW	15

Note. — 1 - Asada et al. 2002; 2 - Asada et al. 2008; 3 - K. Asada 2008, private communication; 4 - Gabuzda et al. 2004; 5 - Gabuzda 2006; 6 - Gabuzda et al. 2008; 7 - Gómez et al. 2008; 8 - Hallahan & Gabuzda 2009; 9 - Mahmud & Gabuzda 2008; 10 - Mahmud & Gabuzda 2009; 11 - O’Sullivan & Gabuzda 2009; 12 - Taylor 1998; 13 - Taylor 2000; 14 - Zavala & Taylor 2002; 15 - Zavala & Taylor 2003; 16 - Zavala & Taylor 2004; 17 - Zavala & Taylor 2005; 18 - Mahmud et al. 2009; 19 - Kharb et al. 2009